SCIENTIFIC REPORTS

OPEN

Cyclic permutations for qudits in *d* dimensions

Tudor-Alexandru Isdrailă[1], Cristian Kusko[2] & Radu Ionicioiu[1]

Received: 19 December 2018
Accepted: 2 April 2019
Published online: 19 April 2019

One of the main challenges in quantum technologies is the ability to control individual quantum systems. This task becomes increasingly difficult as the dimension of the system grows. Here we propose a general setup for cyclic permutations X_d in d dimensions, a major primitive for constructing arbitrary qudit gates. Using orbital angular momentum states as a qudit, the simplest implementation of the X_d gate in d dimensions requires a single quantum sorter S_d and two spiral phase plates. We then extend this construction to a generalised $X_d(p)$ gate to perform a cyclic permutation of a set of d, equally spaced values $\{|\ell_0\rangle, |\ell_0+p\rangle, \ldots, |\ell_0+(d-1)p\rangle\} \mapsto \{|\ell_0+p\rangle, |\ell_0+2p\rangle, \ldots, |\ell_0\rangle\}$. We find compact implementations for the generalised $X_d(p)$ gate in both Michelson (one sorter S_d, two spiral phase plates) and Mach-Zehnder configurations (two sorters S_d, two spiral phase plates). Remarkably, the number of spiral phase plates is independent of the qudit dimension d. Our architecture for X_d and generalised $X_d(p)$ gate will enable complex quantum algorithms for qudits, for example quantum protocols using photonic OAM states.

All successful technologies are based on harnessing a specific resource, such as energy, electricity or information. The ability to generate, control, transform and ultimately, find useful applications for quantum resources, is central to the development of quantum technologies[1–4].

Controlling the simplest quantum systems, the qubit, is relatively straightforward[5,6]. We can achieve complete control over the 2-dimensional Hilbert space of a qubit with rotations generated by Pauli matrices X and Z. The natural next step is to go to d-dimensional systems, or qudits. In this case we have the generalised Pauli matrices X_d and Z_d. Progressing in this direction, we need to find physical implementations for qudits, together with the experimental ability to control them.

Orbital angular momentum (OAM) is one of the most used implementations for photonic qudits. Photon states $|\ell\rangle$ carry an OAM of $\ell\hbar$, where $\ell = 0, \pm 1, \pm 2, \ldots$ is a theoretically unbounded integer. OAM states have a helical phase front, with $\ell \neq 0$ corresponding to the number of helices.

Photonic OAM states have been used in entanglement generation[7–9] and alignment-free quantum key distribution[10,11]. Thus OAM is attractive since it allows us to use a larger alphabet to transmit quantum information with a single photon. However, without the appropriate tools, a larger alphabet for encoding information has only a limited functionality. This brings us to the problem of how to implement efficiently the generalised Pauli operators X_d and Z_d for qudits[12].

For photonic OAM states, Z_d can be implemented with Dove prisms. An open question is how to implement a cyclic permutation X_d for any dimension d. Experimentally, cyclic X_d gates for OAM states have been realised only for $d = 4$[13] and $d = 5$[14].

In this article we propose a general scheme to perform cyclic permutations X_d for any set of d consecutive states. We then generalise it for cyclic permutations $X_d(p)$ of an arbitrary set of d, equally spaced states $\{|\ell_0\rangle, |\ell_0 + p\rangle, \ldots, |\ell_0 + (d-1)p\rangle\}$. For any dimension d, the minimal implementation of both X_d and $X_d(p)$ requires a single sorter S_d and two spiral phase plates (SPPs)[15–18]. To arrive at this setup, we use quantum information methods and quantum network analysis. This approach has been employed previously to design a universal quantum sorter[19] and spin measuring devices[20,21].

We focus on OAM encoded qudits, as several experimental tools are already available[22–28]. Nevertheless, our scheme can be extended in principle to other degrees of freedom as well.

[1]Horia Hulubei National Institute of Physics and Nuclear Engineering, Bucharest–Măgurele, 077125, Romania. [2]National Institute for Research and Development in Microtechnologies IMT, Bucharest, 077190, Romania. Correspondence and requests for materials should be addressed to R.I. (email: r.ionicioiu@theory.nipne.ro)

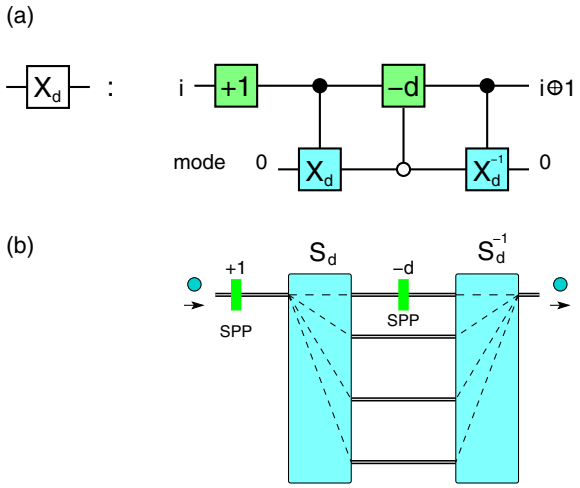

Figure 1. Cyclic X_d gate. The gate performs the transformation $|i\rangle \mapsto |i \oplus 1\rangle$ on a qudit. (**a**) Equivalent quantum network. Spatial modes are used as a qudit ancilla, which is factorised before and after the gate, i.e., starts and ends up in the state $|0\rangle_m$. There are two SPPs of order $+1$ and $-d$ (green) and two $C(X_d)$ gates (cyan). The SPP($-d$) acts only on mode 0 (open circle on the control mode qudit). (**b**) Implementation. Photons enter from the left and all OAM states are shifted by SPP($+1$). The sorter S_d redirects each state to the corresponding output. The state $|d\rangle_{OAM}$ exits on spatial mode 0 and after the SPP($-d$) becomes $|0\rangle_{OAM}$; all other OAM states $|j\rangle$, $j \neq d$, are left invariant. Finally, all states enter the inverse sorter S_d^{-1} and end up in the same spatial mode $|0\rangle_m$.

Results

Cyclic X_d gate. We now introduce our setup for performing the cyclic gate. Let $\mathcal{H}_d$ be the Hilbert space of a qudit, $\dim \mathcal{H}_d = d$ and let $\{|j\rangle\}_{j=0}^{d-1}$ be an orthonormal basis of $\mathcal{H}_d$. The generalised Pauli operators X_d, Z_d are defined as:

$$X_d: \quad |j\rangle \mapsto |j \oplus 1\rangle \tag{1}$$

$$Z_d: \quad |j\rangle \mapsto \omega^j |j\rangle \tag{2}$$

with $\oplus$ addition mod d and $\omega = e^{2\pi i/d}$ a root of unity of order d. The gate X_d performs a cyclic permutation of the basis states, i.e., maps the set $\{|0\rangle, |1\rangle, \ldots, |d-1\rangle\}$ to $\{|1\rangle, |2\rangle, \ldots, |0\rangle\}$.

Our scheme for the X_d gate is shown in Fig. 1. The main element of our proposal is a d-dimensional sorter S_d introduced in refs[19,29]. A quantum sorter S_d is a device which directs an incoming particle into different outputs (i.e., sorts) according to the value of an internal degree of freedom Σ. In the following we take Σ to be orbital angular momentum (OAM). Nevertheless, the setup is general and can be implemented for other variables as well, like wavelength[19] or radial quantum number[30,31].

The quantum sorter S_d is formally equivalent to a controlled-X_d gate between the degree of freedom we want to sort (OAM, Σ etc) and spatial modes m, see Fig. 2:

$$S_d := C(X_d): \quad |i\rangle_{OAM}|j\rangle_m \mapsto |i\rangle_{OAM}|j \oplus i\rangle_m \tag{3}$$

where $|i\rangle_{OAM}, |j\rangle_m$ are OAM and mode qudits, respectively. Thus a photon in OAM state $|i\rangle$ incident on port (mode) 0 will exit on port ($i \bmod d$) with unit probability.

Apart from the sorter S_d another ingredient are spiral phase plates[15–18] of order n. The action of the SPP on OAM states is:

$$\text{SPP}(n): \quad |i\rangle_{OAM} \mapsto |i + n\rangle_{OAM} \tag{4}$$

with $n \in \mathbb{Z}$ integer. This transformation adds (or subtracts) n units of OAM. Since this is normal addition, it shifts the whole $\mathbb{Z}$ axis by n units.

We now discuss how the X_d gate in Fig. 1 works. The first SPP adds $+1$ to all OAM states. Then the sorter S_d directs each OAM state $|i\rangle_{OAM}$ to the corresponding output $|i \bmod d\rangle_m$, eq. (3). Since sorting on modes is done modulo d, the state $|d\rangle_{OAM}$ will exit on mode 0. Consequently, only the state on mode 0 needs to be shifted by $-d$; in terms of quantum networks, this is equivalent to a controlled-SPP($-d$) gate, with the control on the mode $k = 0$ (open circle on control qudit in Fig. 1). After this operation the states from all spatial modes are recombined on mode 0 by the gate $C(X_d)^{-1}$, which is nothing else but a sorter run in reverse S_d^{-1}. This decouples the OAM and mode qudits, such that the final state is factorised and the photon always exits on mode 0 with unit probability. Thus the gate in Fig. 1 performs the following sequence:

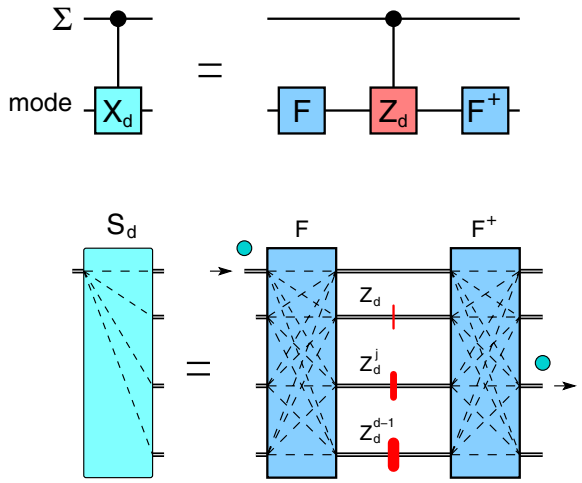

Figure 2. Universal quantum sorter S_d. Top: equivalent quantum network. The controlled-X_d gate $C(X_d)$ is decomposed on Fourier gates F, $F^\dagger$ and a $C(Z_d)$ gate. Bottom: implementation as a multimode interferometer with path-dependent phase shifts Z_d^j acting on the variable to be sorted Σ.

	SPPs	Fourier F	Z_d phases
Resources	2	4, integrated optics $O(d^2)$, linear optics $O(\frac{d}{2}\log d)$, if $d=2^p$	$2(d-1)$

Table 1. Resource scaling for the cyclic X_d gate.

$$
\begin{aligned}
|i\rangle_{OAM}|0\rangle_m &\xrightarrow{+1} |i+1\rangle_{OAM}|0\rangle_m \\
&\xrightarrow{S_d} |i+1\rangle_{OAM}|i\oplus 1\rangle_m \\
&\xrightarrow{-d^{[0]}} |i\oplus 1\rangle_{OAM}|i\oplus 1\rangle_m \\
&\xrightarrow{S_d^{-1}} |i\oplus 1\rangle_{OAM}|0\rangle_m
\end{aligned} \tag{5}
$$

Since the ancilla is decoupled after the gate, an arbitrary superposition of OAM states transforms under the cyclic gate X_d as

$$\alpha_0|0\rangle + \alpha_1|1\rangle + \ldots + \alpha_{d-1}|d-1\rangle \rightarrow \alpha_{d-1}|0\rangle + \alpha_0|1\rangle + \ldots + \alpha_{d-2}|d-1\rangle \tag{6}$$

Consequently, our scheme preserves coherence and can be used in arbitrary quantum algorithms.

Resources. Our implementation of the cyclic X_d gate requires two sorters S_d and two SPPs (of order $+1$ and $-d$, respectively). This result is important: the number of SPPs is constant (two), and thus independent of the qudit dimension d. A Michelson configuration simplifies this to a single sorter and two SPPs, see section below.

Each sorter S_d requires $d-1$ phases Z_d (on OAM) and two Fourier gates F_d, $F_d^\dagger$ on spatial modes[19], Fig. 2. Fourier gates for spatial modes[32–35] can be implemented in several ways.

In integrated optics the Fourier gate is performed by a single slab coupler[36], e.g., as used in arrayed waveguide gratings (AWG)[37]. Commercially available AWGs containing Fourier gates have tens to hundreds of spatial modes (channels).

In bulk optics the Fourier transform can be implemented with a pair of confocal lenses with waveguides attached[36]. Alternatively, the Fourier gate can be decomposed in $O(d^2)$ linear optics elements (beamsplitters and phase-shifters)[34,38,39]. For $d = 2^p$, $p \in \mathbb{N}$, the Fourier transform on d modes can be implemented with $O(\frac{d}{2}\log d)$ linear optical elements (beamsplitters and phase-shifters)[32,40]. The resource scaling for the X_d gate is summarised in Table 1.

We now briefly discuss possible implementations. Given the scaling discussed above and the current advances in photonics, we expect to have sizes $d \sim 5-10$ in bulk optics and $d \sim 100$ in integrated photonics.

Generalised X_d gate. The previous setup implements a cyclic X_d gate on the set $\{|0\rangle, |1\rangle, \ldots, |d-1\rangle\}$. We now discuss two generalisations.

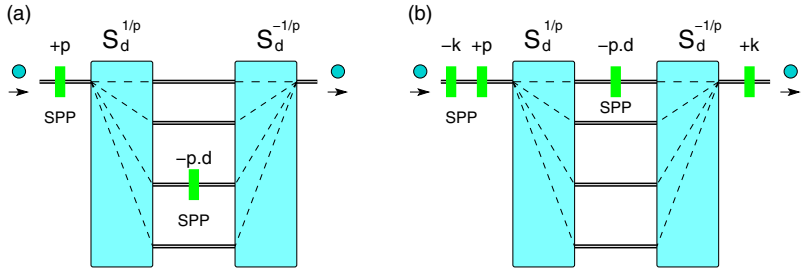

Figure 3. Generalised cyclic gate $X_d(p)$. The gate performs a cyclic permutation on the set $\{|\ell_0\rangle, |\ell_0 + p\rangle, \ldots, |\ell_0 + (d-1)p\rangle\}$. There are two ways to correct for the initial state ℓ_0: (**a**) by moving SPP($-pd$) to spatial mode k, with $k = \ell_0 \bmod d$; (**b**) by inserting before and after the sorters two SPPs, SPP($-k$) and SPP(k). Note that $0 \leq k < d$.

(i) Cyclic permutation for d consecutive values. The first generalisation is to perform a cyclic X_d gate on an arbitrary set of d consecutive OAM values $\{|\ell_0\rangle, |\ell_0 + 1\rangle, \ldots, |\ell_0 + d - 1\rangle\}$. From the general transformation of the sorter, we know that a state with OAM ℓ_0, incident on spatial mode 0, will exit on spatial mode $k = \ell_0 \bmod d$. Thus the only modification of the scheme in Fig. 1 is to move SPP($-d$) from mode 0 to mode k, Fig. 3(a).

A second method to perform the cyclic X_d gate on the set $\{|\ell_0\rangle, |\ell_0 + 1\rangle, \ldots, |\ell_0 + d - 1\rangle\}$ is to first shift all OAM states with $-k$, then perform the usual X_d gate, and finally shift back all states with $+k$, Fig. 3(b).

Importantly, the value of the shift k is bounded by the dimension d of the qudit and not by ℓ_0, since $0 \leq k < d$. This is noteworthy – although OAM with large values $\ell = 10010$ have been experimentally prepared[41], SPPs with such large values are very difficult to manufacture. Therefore, for $\ell \gg d$ we need to shift the state only with a much smaller value $(\ell_0 \bmod d) < d$, irrespective of the magnitude of ℓ_0. Thus the same device can be used to perform the cyclic X_d gate on any set of d consecutive OAM states. In this case the only change is the position of SPP($-d$) (for the first method), or adding two extra SPP($\pm k$) (for the second method).

(ii) Cyclic permutation for d, equally spaced values. Let $p \in \mathbb{N}^+$ be a positive integer. We now show how to implement a cyclic permutation with step p

$$\{|0\rangle, |p\rangle, \ldots, |(d-1)p\rangle\} \mapsto \{|p\rangle, |2p\rangle, \ldots, |0\rangle\} \tag{7}$$

We define the generalised gate $X_d(p)$

$$X_d(p): \quad |jp\rangle \mapsto |(j \oplus 1)p\rangle \tag{8}$$

with $j = 0, \ldots, d-1$, $p \in \mathbb{N}^+$ and $\oplus$ addition mod d. The gate is characterised by two parameters: the qudit dimension d and the step p between two consecutive values; clearly $X_d(1) = X_d$.

The implementation of $X_d(p)$ uses the same architecture as before, but with a different sorter $S_d^{1/p}$: this directs each state $|jp\rangle_{OAM}$ on a separate mode $|j\rangle_m$. From the decomposition $S_d^{1/p} = F^\dagger C(Z_d^{1/p})F$, it follows that we can implement $S_d^{1/p}$ with a setup similar to Fig. 2, but with different mode-dependent phases $Z_d^{j/p}$ inside the interferometer.

The setup for $X_d(p)$ is shown in Fig. 3. As before, SPP(p) first shift all OAM states with p. The sorter $S_d^{1/p}$ separates the states according to the OAM values, $|jp\rangle_{OAM}|0\rangle_m \mapsto |jp\rangle_{OAM}|j\rangle_m$. Then SPP($-pd$) maps $|dp\rangle_{OAM} \mapsto |0\rangle_{OAM}$, after which the sorter $S_d^{-1/p}$ combines back all states on mode $|0\rangle_m$.

As before, we can implement a cyclic gate $X_d(p)$ on an arbitrary set of equally spaced OAM values $\{|\ell_0\rangle, |\ell_0 + p\rangle, \ldots, |\ell_0 + (d-1)p\rangle\}$ in two ways, Fig. 3:

(a) by moving SPP($-pd$) on mode k, with $k = \ell_0 \bmod d$; or
(b) by using two SPP($\pm k$) before and after the sorters.

To summarise, for any dimension d and initial state ℓ_0, the generalised gate $X_d(p)$ requires only two sorters $S_d^{1/p}, S_d^{-1/p}$ and two spiral phase plates SPP(p), SPP($-pd$).

Simplification: Michelson setup. We can further simplify our scheme if we use a Michelson instead of the Mach-Zehnder interferometer. In this case we need only one sorter $S_d^{1/p}$, Fig. 4. The first part of the scheme is identical to the one discussed previously. The state $|dp\rangle_{OAM}$ exits on spatial mode k and, after a reflection on SPP($-pd$), becomes $|0\rangle_{OAM}$. All other OAM states undergo a double reflection on the retro-reflector R and remain unchanged. Finally, all states re-enter the sorter from the opposite direction, thus performing $S_d^{-1/p}$, and end up in the same spatial mode $|0\rangle_m$. A circulator C separates the output from the input. Note that a spiral phase plate acts as its inverse if the photon enters from the opposite direction; thus in Fig. 4(b) we need only a single SPP($-k$).

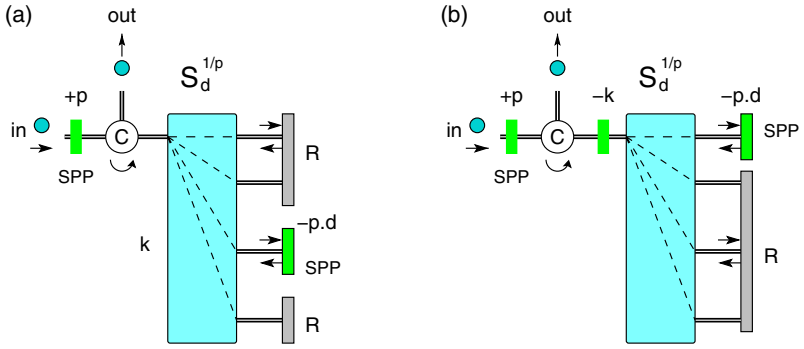

Figure 4. Michelson interferometer configuration for $X_d(p)$ gate. This is the folded version of the Mach-Zehnder setup in Fig. 3. The state $|dp\rangle_{OAM}$ exits on spatial mode 0 and after a reflection on SPP($-pd$) becomes $|0\rangle_{OAM}$. All other OAM states $|jp\rangle_{OAM}$, $j \neq d$, are left invariant by a double reflection on retro-reflectors R. Subsequently, all states re-enter the sorter from the opposite direction, thus performing $S_d^{-1/p}$, and end up in the same spatial mode $|0\rangle_m$. A circulator C separates the output from the input. Cases (**a** and **b**) are equivalent to Fig. 3(a,b), respectively.

Discussion

The ability to control higher-dimensional quantum systems is essential for developing useful quantum technologies. Due to coherence constraints, efficiency will play a key role in the success of real-life quantum protocols. In this article we designed implementations for cyclic permutations X_d in d dimensions, one of the building blocks for constructing arbitrary single-qudit gates. The scheme is deterministic, works at single-particle level and can be applied to arbitrary superpositions of qudit states. Regarding the resource scaling, both X_d and $X_d(p)$ gates require a linear number of phase-shifts Z_d. Remarkably, for any dimension d the number of spiral phase plates SPPs is two, thus constant.

Although our focus has been on orbital angular momentum, the method is general and can be adapted to other degrees of freedom. This will require a sorter S_d and shift gates (the equivalent of SPP) for the respective degree of freedom. Since a general scheme for a universal quantum sorter exists[19], a future challenge to implement the cyclic gate X_d for a particular degree of freedom Σ is to find appropriate implementations for shift gates $|i\rangle_\Sigma \mapsto |i+n\rangle_\Sigma$.

A possible application of the generalised cyclic permutation $X_d(p)$ is quantum communication, e.g., in QKD protocols with Fibonacci coding for key distribution[42,43].

Note added. While finishing this article we became aware of another method for performing X_d gates for OAM[44].

References

1. Feynman, R. P. Simulating physics with computers. *Int. J. Theor. Phys.* **21**, 467 (1982).
2. DiVincenzo, D. P. The Physical Implementation of Quantum Computation. *Fortschr. Phys.* **48**, 771 (2000).
3. Dowling, J. P. & Milburn, G. J. Quantum technology: the second quantum revolution. *Phil. Trans. R. Soc. Lond. A* **361**, 1655 (2003).
4. Gisin, N., Ribordy, G., Tittel, W. & Zbinden, H. Quantum cryptography. *Rev. Mod. Phys.* **74**, 145–195 (2002).
5. Barenco, A. *et al.* Elementary gates for quantum computation. *Phys. Rev. A* **52**, 3457 (1995).
6. Nielsen, M. & Chuang, I. L. *Quantum Computation and Quantum Information* (Cambridge University Press, 2010).
7. Mair, A., Vaziri, A., Weihs, G. & Zeilinger, A. Entanglement of the orbital angular momentum states of photons. *Nature* **412**, 313 (2001).
8. Fickler, R. *et al.* Quantum entanglement of high angular momenta. *Science* **338**, 640–643 (2012).
9. Krenn, M. *et al.* Generation and confirmation of a (100 × 100)-dimensional entangled quantum system. *PNAS* **111**, 6243 (2014).
10. D'Ambrosio, V. *et al.* Complete experimental toolbox for alignment-free quantum communication. *Nat. Commun.* **3**, 961, https://doi.org/10.1038/ncomms1951 (2012).
11. Vallone, G. *et al.* Free-Space Quantum Key Distribution by Rotation-Invariant Twisted Photons. *Phys. Rev. Lett.* **113**, 060503 (2014).
12. Bertlmann, R. A. & Krammer, P. Bloch vectors for qudits. *J. Phys. A: Math. Theor.* **41**, 235303 (2008).
13. Schlederer, F., Krenn, M., Fickler, R., Malik, M. & Zeilinger, A. Cyclic transformation of orbital angular momentum modes. *New J. Phys.* **18**, 043019 (2016).
14. Chen, D.-X. *et al.* Realization of quantum permutation algorithm in high dimensional Hilbert space. *Chinese Physics B* **26**, 060305 (2017).
15. Beijersbergen, M. W., Coerwinkel, R. P. C., Kristensen, M. & Woerdman, J. P. Helical-wavefront laser beams produced with a spiral phaseplate. *Opt. Comm.* **112**(5–6), 321 (1994).
16. Allen, L., Padgett, M. J. & Babikera, M. The Orbital Angular Momentum of Light. *Progress in Optics* **39**, 291 (1999).
17. Oemrawsingh, S. S. R. *et al.* Production and characterization of spiral phase plates for optical wavelengths. *Appl. Opt.* **43**, 688 (2004).
18. Wang, X. *et al.* Recent advances on optical vortex generation. *Nanophotonics* **7**, 1533 (2018).
19. Ionicioiu, R. Sorting quantum systems efficiently. *Sci. Rep.* **6**, 25356 (2016).
20. Ionicioiu, R. & D'Amico, I. Mesoscopic Stern-Gerlach device to polarize spin currents. *Phys. Rev. B* **67**, 041307(R) (2003).
21. Ionicioiu, R. & Popescu, A. E. Single-spin measurement using spin-orbital entanglement. *New J. Phys.* **7**, 120 (2005).
22. Leach, J., Padgett, M. J., Barnett, S. M., Franke-Arnold, S. & Courtial, J. Measuring the orbital angular momentum of a single photon. *Phys. Rev. Lett.* **88**, 257901 (2002).
23. Leach, J. Interferometric methods to measure orbital and spin, or the total angular momentum of a single photon. *Phys. Rev. Lett.* **92**, 013601 (2004).

24. Giovannini, D. *et al*. Characterization of high-dimensional entangled systems via mutually unbiased measurements. *Phys. Rev. Lett.* **110**, 143601 (2013).
25. Berkhout, G. C. G., Lavery, M. P. J., Courtial, J., Beijersbergen, M. W. & Padgett, M. J. Efficient sorting of orbital angular momentum states of light. *Phys. Rev. Lett.* **105**, 153601 (2010).
26. Mirhosseini, M., Malik, M., Shi, Z. & Boyd, R. W. Efficient separation of the orbital angular momentum eigenstates of light. *Nat. Commun.* **4**, 2781, https://doi.org/10.1038/ncomms3781 (2013).
27. Babazadeh, A. *et al*. High-dimensional single-photon quantum gates: concepts and experiments. *Phys. Rev. Lett.* **119**, 180510 (2017).
28. Fontaine, N. K. *et al*. Laguerre-Gaussian mode sorter, https://arxiv.org/abs/1803.04126v2.
29. Zou, X. B. & Mathis, W. Scheme for optical implementation of orbital angular momentum beam splitter of a light beam and its application in quantum information processing. *Phys. Rev. A* **71**, 042324 (2005).
30. Zhou, Y. *et al*. Sorting Photons by Radial Quantum Number. *Phys. Rev. Lett.* **120**, 103601 (2017).
31. Gu, X., Krenn, M., Erhard, M. & Zeilinger, A. Gouy Phase Radial Mode Sorter for Light: Concepts and Experiments. *Phys. Rev. Lett.* **120**, 103601 (2018).
32. Barak, R. & Ben-Aryeh, Y. Quantum fast Fourier transform and quantum computation by linear optics. *J. Opt. Soc. Am. B* **24**, 231 (2007).
33. Takiguchi, K., Oguma, M., Shibata, T. & Takahashi, H. Demultiplexer for optical orthogonal frequency-division multiplexing using an optical fast-Fourier-transform circuit. *Opt. Lett.* **34**, 1828 (2009).
34. Tabia, G. N. M. Recursive multiport schemes for implementing quantum algorithms with photonic integrated circuits. *Phys. Rev. A* **93**, 012323 (2016).
35. Kita, D. M. *et al*. High-performance and scalable on-chip digital Fourier transform spectroscopy. *Nat. Commun.* **9**, 4405, https://doi.org/10.1038/s41467-018-06773-2 (2018).
36. Cincotti, G. What else can an AWG do? *Opt. Express* **20**, B288 (2012).
37. Lowery, A. J. Design of arrayed-waveguide grating routers for use as optical OFDM demultiplexers. *Opt. Express* **18**, 14129 (2010).
38. Reck, M., Zeilinger, A., Bernstein, H. J. & Bertani, P. Experimental realization of any discrete unitary operator. *Phys. Rev. Lett.* **73**, 58 (1994).
39. Clements, R. W., Humphreys, P. C., Metcalf, B. J., Kolthammer, W. S. & Walmsley, I. A. Optimal design for universal multiport interferometers. *Optica* **3**, 1460 (2016).
40. Crespi, A. *et al*. Suppression law of quantum states in a 3D photonic fast Fourier transform chip. *Nat. Commun.* **7**, 10469, https://doi.org/10.1038/ncomms10469 (2016).
41. Fickler, R., Campbell, G., Buchler, B., Lam, P. K. & Zeilinger, A. Quantum entanglement of angular momentum states with quantum numbers up to 10,010. *PNAS* **113**, 13642 (2016).
42. Simon, D. S. *et al*. High-capacity quantum Fibonacci coding for key distribution. *Phys. Rev. A* **87**, 032312 (2013).
43. Pan, Z., Cai, J. & Wang, C. Quantum Key Distribution with High Order Fibonacci-like Orbital Angular Momentum States. *Int. J. Theor. Phys.* **56**, 2622 (2017).
44. Gao, X., Krenn, M., Kysela, J. & Zeilinger, A. Arbitrary *d*-dimensional Pauli *X* Gates of a flying Qudit. *Phys. Rev. A* **99**, 023825 (2019).

Acknowledgements

The authors acknowledge support from a grant of the Romanian Ministry of Research and Innovation, PCCDI-UEFISCDI, project number PN-III-P1-1.2-PCCDI-2017-0338/79PCCDI/2018, within PNCDI III. R.I. acknowledges support from PN 18090101/2018.

Author Contributions

C.K. and R.I. proposed the theoretical method. T.A.I. and R.I. wrote the manuscript. All authors reviewed the manuscript.

Additional Information

Competing Interests: The authors declare no competing interests.

Publisher's note: Springer Nature remains neutral with regard to jurisdictional claims in published maps and institutional affiliations.